

CHAPTER III

EXPERIMENTAL PROCEDURE

3.1 Preparation of Test Specimens

The schematic drawings of process to make ingot and test pieces are shown in Fig.3-1. The charge calculations are carried out for the target chemical compositions of hypoeutectic 16% Cr cast irons. As raw materials, mild steel scrap, pig iron, ferro-alloys, pure metals are used. The total weight of 30 kg of charge materials is melted down in a high frequency induction furnace with alumina (Al_2O_3) lining and superheated up to 1853 K (1580 °C). After holding, the melt is poured at 1773-1793 K (1500-1520 °C) into the preheated CO_2 mold in Y-block shape of which cavity size of specimen is 50x50x200 mm. After pouring, the melt is immediately covered with dry exothermic powder to hold the temperature of riser (Fig.3-1(a)). The chemical compositions of the test specimens are summarized in Table 3-1.

Table 3-1 Chemical composition of specimens.

Specimens		Alloy (mass%)				
		C	Cr	Si	Mn	Mo
No.1	Aim	3.00	16.00	0.50	0.55	0.00
	Chemistry	2.96	15.93	0.51	0.55	0.22
No. 2	Aim	3.00	16.00	0.50	0.55	1.00
	Chemistry	2.95	16.00	0.50	0.55	1.06
No.3	Aim	3.00	16.00	0.50	0.55	3.00
	Chemistry	2.91	15.91	0.47	0.55	2.98

The rizer part was cut off from Y-block ingot and the substantial block is supplied for annealing to remove the casting stress and micro-segregation produced during solidification. The substantial block is coated with an anti-oxidation solution to prevent the block from oxidation and decarburization. The block in an electric furnace was heated up from room temperature to 1173 K (900°C) with a heating rate of 0.1 K/s and held for 18 ks (5 hours) and follow by cooling in the furnace to the room temperature. In order to make test pieces for abrasion wear test, the block was sliced into pieces with 7 mm in thickness using a wire-cut machine called EDM (Electric Discharge Machine). The process of making test pieces is shown in Fig. 3-1(c).

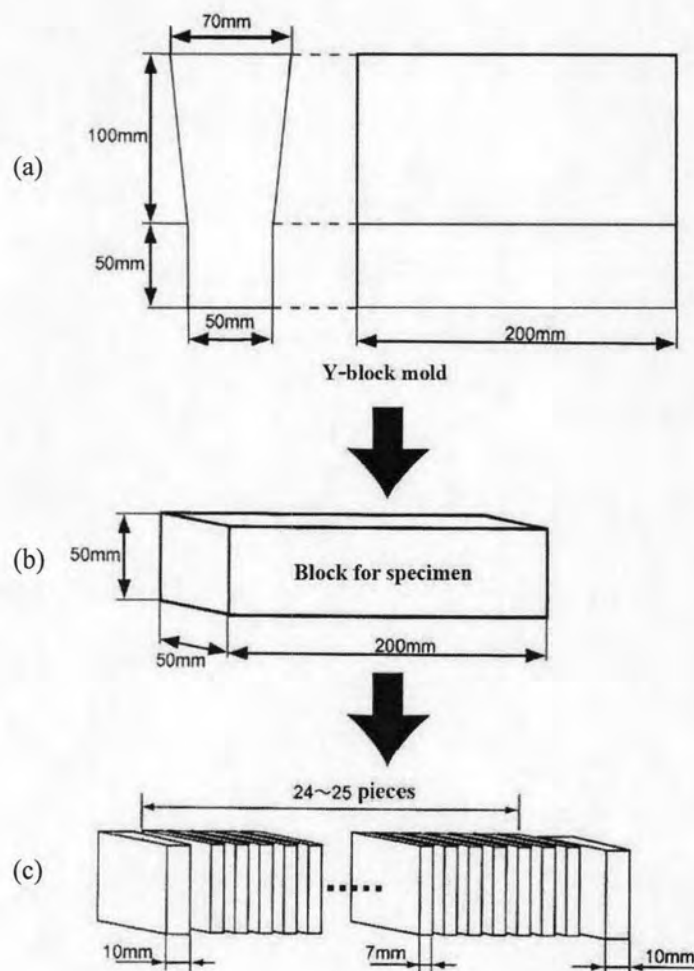


Fig.3-1 Process of making test pieces.

3.2 Heat Treatment Conditions

The conditions of heat treatment are listed in Table 3-2.

3.2.1 Hardening

The sliced test pieces were also coated by the anti-oxidation solution and dried at 473K (200°C) in an electric furnace. They were heated up to 1323 K (1050 °C) for austenitization. After holding for 5.4 ks (1.5 hours), the test pieces are hardened by fan air cooling.

3.2.2 Tempering

The hardened test pieces are tempered in a furnace at 3 levels of temperatures from 673 to 873 K. The tempering temperatures were determined according to the reference [8] and they are shown in Table 3-3. After tempering, the test pieces are cooled to the room temperature by fan air cooling.

Table 3-2 Heat treatment condition.

Heat Treatment	Annealing	Hardening	Tempering
Temperature (K)	1173	1323	3 levels between
Holding Time (ks)	18.0	5.4	7.2
Cooling Condition	Furnace Cooling	Fan Air Cooling	Fan Air Cooling

Table 3-3 Tempering temperature.

Specimens	Tempering Temperature* (K)		
	Before H_{Tmax}	H_{Tmax}	Over H_{Tmax}
No. 1 (16%Cr alloy-free)	673	748	773
No. 2 (16%Cr -1%Mo)	673	798	823
No. 3 (16%Cr -3%Mo)	673	823	873

The reason why there tempering temperatures for specimens were introduced is explained as follows.

The relationship between macro-hardness and tempering temperature is schematically illustrated in Fig.3-2. Tempering temperatures were selected by referring to the reference[8], those before $H_{T_{max}}$ ($673K$) ($B-H_{T_{max}}$) of which case has high retained austenite (V_{γ}), $H_{T_{max}}$ and over $H_{T_{max}}$ ($O-H_{T_{max}}$) of which case has little V_{γ} by referring to the reference[8].

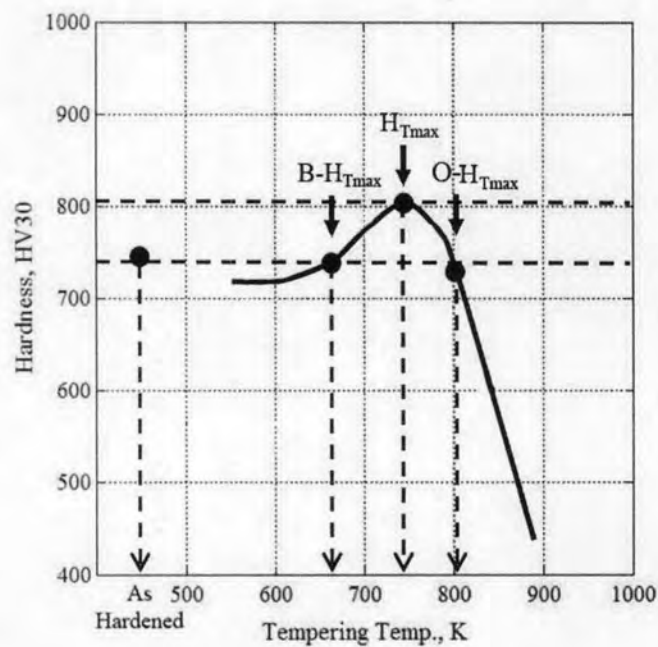


Fig.3-2 Schematic drawing to select tempering temperatures.

3.3 Observation of Microstructure

3.3.1 Optical microscope (OM)

To observe the microstructure by means of an optical microscope (OM), the specimen is polished using emery papers in the order of #180, 320, 400 and 600 and finished by a buff cloth with extremely fine alumina powder of $0.3 \mu\text{m}$ in diameter. The microstructure is revealed using an etchants shown in Table 3-4.

Table 3-4 List of etchants.

Type	Etchant	Etching method	Attack
A	Picric acid 1 g + HCl 5 cc + Ethanol 100 cc	Immersion at room temperature	Carbide and matrix
B	HNO ₃ 5 cc + Ethanol 95 cc	Immersion at room temperature	Matrix

3.3.2 Scanning Electron Microscopy (SEM)

For more discussions, the microstructure involving secondarily precipitated carbides are observed by high magnification using a Scanning Electron Microscope (SEM). A polished specimen is lightly etched using the etchant A to reveal the microstructure. The microphotographs focusing on the carbide morphology in matrix are taken by high magnification.

3.3.3 Electron Probe Microanalyzer (EPMA)

In order to confirm the alloy distribution in the matrix, the elements in the as-cast specimens are analyzed by using an Electron Probe Microanalyzer (EPMA). The distributions of Fe, C, Cr and Mo are revealed clearly by the characteristic X-ray images.

3.4 Measurement of Hardness

Macro-hardness of test pieces is measured by means of Vickers hardness tester with applying a load of 297 N (30 kg) and micro-hardness is by Micro-Vickers hardness tester with applying a load of 1 N (100 g). In each test piece, the hardness is measured at five different places and their average value is adopted.

3.5 Measurement of Volume Fraction of Austenite(V_γ)

3.5.1 Theory for measurement of austenite by X-ray diffraction method

Quantitative measurement of austenite in matrix is not so easy because a bulk test piece with different orientation of dendrites must be used for X-ray diffraction method. In the methods to measure the volume fraction of austenite (V_γ), however, X-ray diffraction method is convenient when the texture is cancelled as if the surface of specimen in powder sample.

The basic equation of diffraction intensity of a phase is expressed as

$$I_{hkl} = K(FF^*)(LPF)me^{-2M}A(\theta)V_i/v_i^2 \quad (\text{Eq.3-1})$$

where, K = proportional constant

FF^* = structure factor of the unit cell of the interest phase, equal to $4f^2$ and $16f^2$ for diffraction lines of α (martensite/ferrite) and γ (austenite), respectively, where f is the atomic-scattering factor of the species of atom which make up the unit cell : f relates to $(\sin \theta)/\lambda$

LPF = Lorenz Polarization Factor, $(1+\cos^2 2\theta)/\sin^2 \theta \cos \theta$

m = multiplicity factor, the number of $\{hkl\}$ planes in a unit cell

e^{-2M} = Debye -Waller temperature factor where

M = $(B \sin^2 \theta) / \lambda^2$: B is a material constant

$A(\theta)$ = absorption factor, independent of θ if sample is flat

V_i = volume fraction of the phase

v_i = volume of unit cell

Let, $K' = K \times A(\theta)$ (Eq.3-2)

and $R_{hkl} = [FF^*(LPF)me^{-2M}]/v_i^2$ (Eq.3-3)

Here, Debye-Waller temperature factor is negligible. Substitute K' and R_{hkl}

in the Eq.3-1 to be Eq.3-4,

$$I_{hkl} = K' R_{hkl} V_i \quad (\text{Eq.3-4})$$

When several peaks in the diffraction pattern participate in the calculation, the above equation is shown by the next Eq.3-5,

$$\sum I_{hkl} = K' (\sum R_{hkl}) (V_i) \quad (\text{Eq.3-5})$$

Therefore, peaks of ferrite and/or martensite (α) and peaks of austenite (γ) are respectively shown as

$$\sum I_{\alpha} = K' (\sum R_{\alpha}) (V_{\alpha}) \quad (\text{Eq.3-6})$$

$$\sum I_{\gamma} = K' (\sum R_{\gamma}) (V_{\gamma}) \quad (\text{Eq.3-7})$$

Besides,

$$V_{\alpha} + V_{\gamma} + V_c = 1 \quad (\text{Eq.3-8})$$

where, V_c is the volume fraction of other phase.

Assume only α and γ phases exist in the specimen, the Eq.3-8 is,

$$V_{\alpha} + V_{\gamma} = 1 \quad (3.9)$$

The relationship between V_{α} and V_{γ} from the Eq.3-6) and Eq.3-7 can be expressed by the next equation,

$$V_{\alpha} = \frac{[\sum I_{\alpha} \cdot \sum R_{\gamma} / \sum I_{\gamma} \cdot \sum R_{\alpha}]}{\alpha} V_{\gamma} \quad (\text{Eq.3.10})$$

Solving the Eq.3-9 and the Eq.3-10 to obtain the volume fraction of austenite which relates to the diffraction peak intensity and R values, the following equation is finally given,

$$V_{\gamma} = \frac{1}{1 + (\alpha \sum I_{\alpha} \cdot \sum R_{\gamma} / \sum I_{\gamma} \cdot \sum R_{\alpha})} \quad (\text{Eq.3.11})$$

For the determination of the amount of austenite, R values must be obtained by Eq.3-3 and I_{α} and I_{γ} values by measuring the areas of the diffraction peaks of α and γ . Resultantly, the volume fraction of austenite (V_{γ}) is obtained numerically.

3.5.2 Equipment and measuring condition

The quantitative measurement of V_γ is carried out using X-ray diffraction method which was developed for steel by R.L. Miller and then for high chromium white iron by C. Kim [6]. The measuring conditions are summarized Table 3-5. In this experiment, the simultaneously rotating and swinging sample stage was employed to cancel the influence of preferred orientation or textural structure of austenite in the cast iron specimen. The sample stage is shown in Fig.3-3. Fig.3-4 illustrates the results of preliminary tests using the same specimens as this experiment. The results prove the advantage of use of the sample stage with rotating and swinging. It is evident that the peaks of γ_{220} and γ_{311} are stronger in the specimen with rotating and swinging (a) than those in the both cases of only rotating (b) and of without both rotating and swinging (c). On the other hand, the peaks of α_{200} and α_{220} are weak when the sample stage with rotating and swinging is used. However, the V_γ calculated from the diffraction peaks measured using the rotating and swinging sample stage is higher than the other cases. It is because the rotating and swinging could cancel the preferred-orientation or texture of austenite. This sample stage is used every time in this research.

For this investigation, the test piece was prepared by grinding surface and followed by polishing it in the same way as the test piece for microphotography. Mo-K α characteristic line with a wavelength of 0.0711 nm (0.711 \AA) was used as a source of X-ray beam.

Table 3-5 Condition of X-ray diffraction method to measure the volume fraction of retained austenite

Target metal	Mo
Tube Voltage · Current	50 kV · 30mA
Slits	Divergence Slit: 1°, Receiving Slit: 1.5 mm, Scattering Slit: 1°
Filter	Zr
Scanning Range	24-44 deg
Scanning Speed	0.5 deg/min
Step/Sampling	0.01 deg

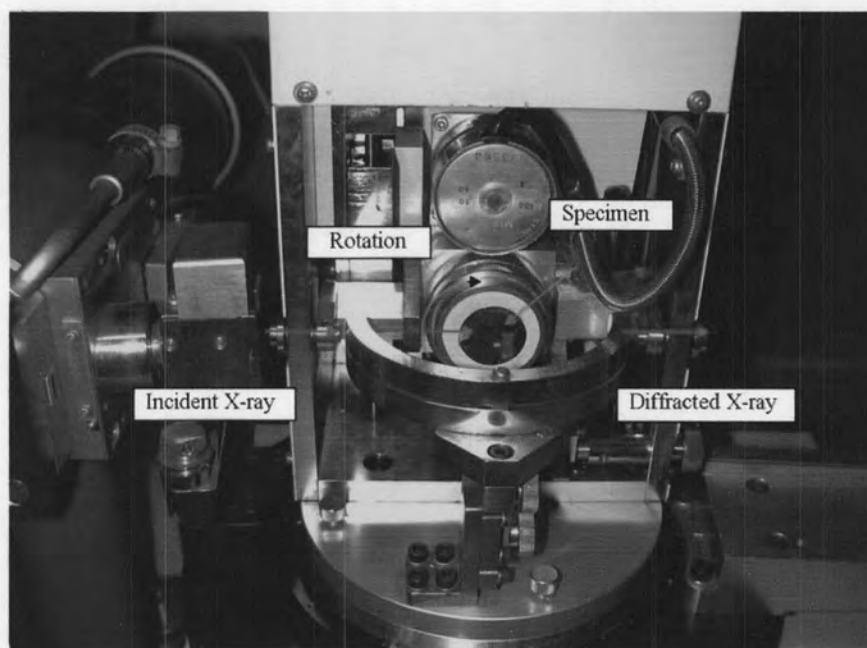
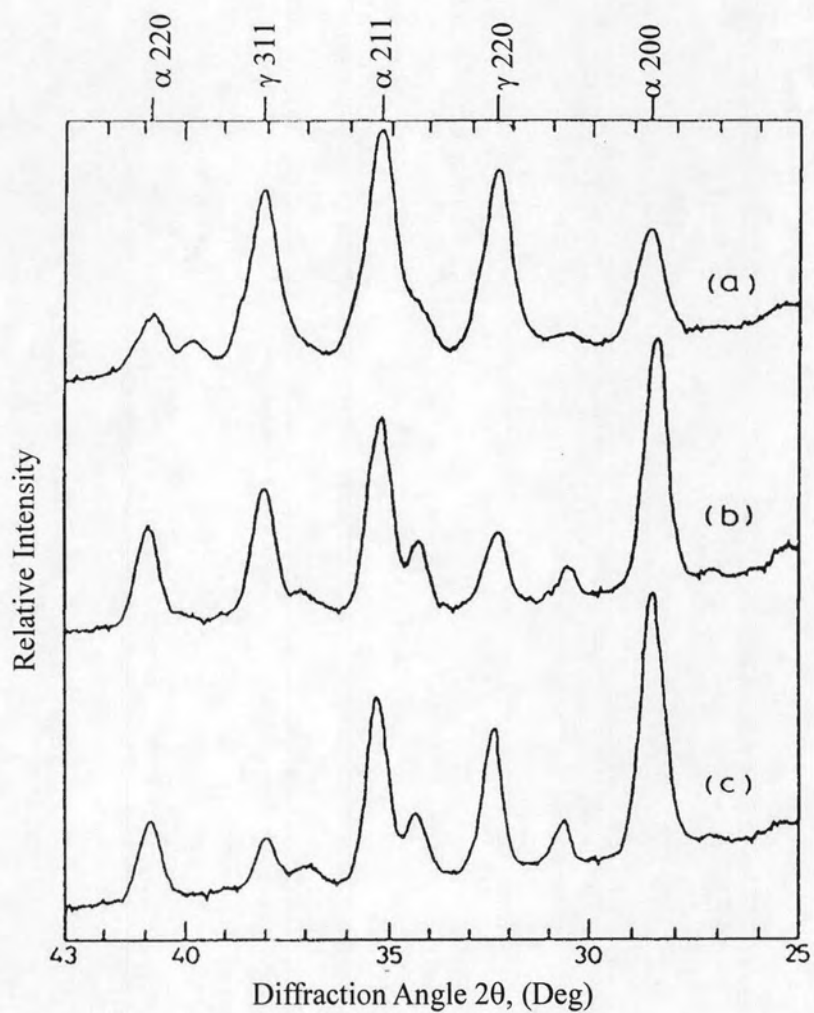


Fig.3-3 Photograph of special sample stage for retained austenite measurement by X-ray diffraction method.



Symbol	Condition	V_γ (%)
(a)	Rotating and swinging	71
(b)	Rotating	37
(c)	Without (a) and (b)	18

Fig.3-4 Effect of sample stage usage on diffraction pattern and volume fraction of retained austenite (V_γ) calculated.

3.5.3 Calculation of volume fraction of austenite

In this investigation, the crystal planes of peaks adopted for the calculation are (200), (220) of ferrite or/and martensite and (220), (311) of austenite because these four peaks are independent or not interfering from peaks of other phases like carbides. The diffraction patterns of three specimens with different V_γ are shown for comparison in Fig.3-5. Reason why the α_{211} peak in these patterns is not taken into account is that this peak is overlapped with a strong peak of chromium carbide. The integrated areas of these peaks are obtained using an image analyzer. The calculation of V_γ is done by the three combination of peaks, $\alpha_{200} - \gamma_{311}$, $\alpha_{200} - \sum\gamma(220,311)$ and $\sum\alpha(200,220) - \gamma_{311}$. The average of values calculated from three combinations is adopted.

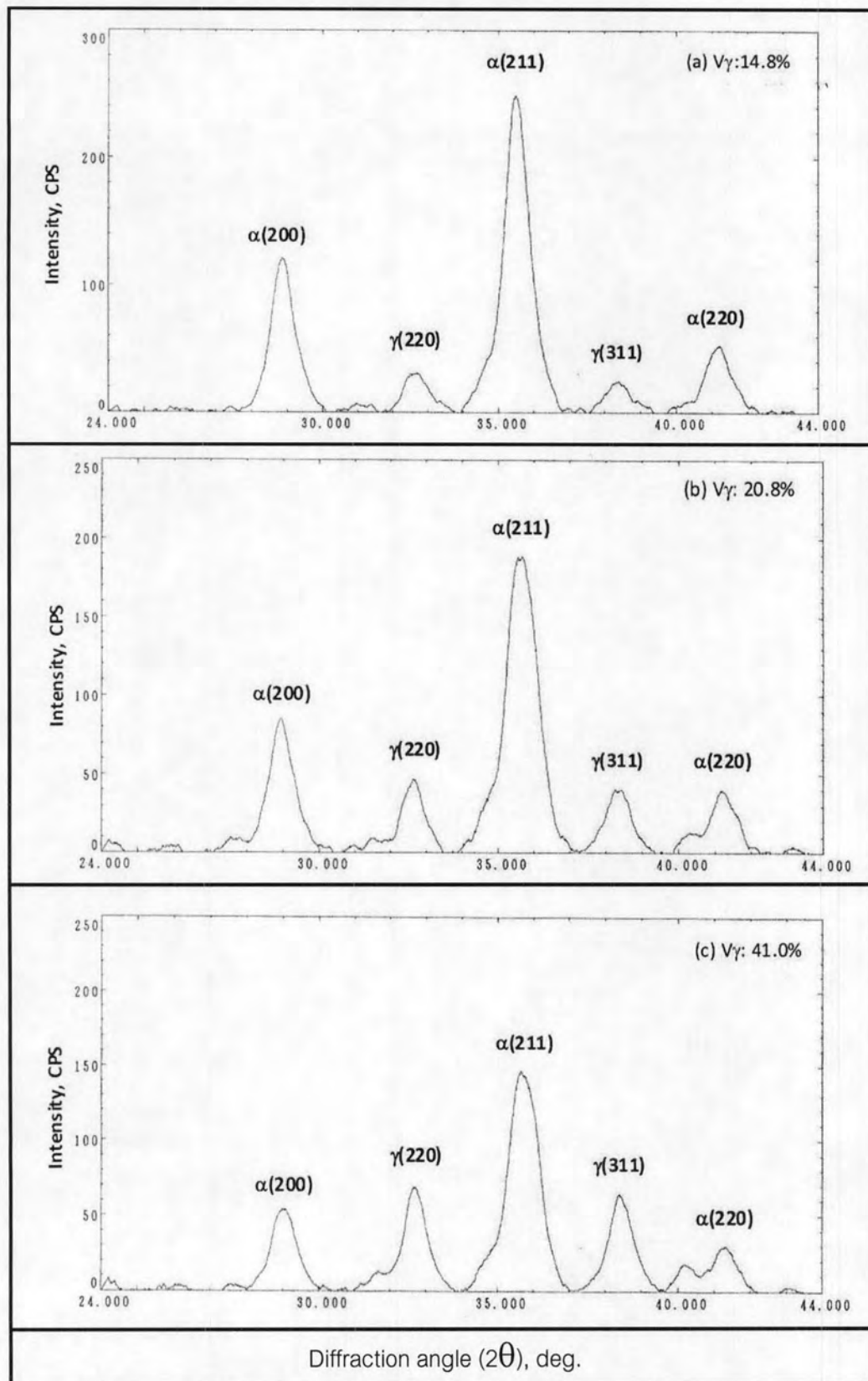


Fig.3-5 X-ray diffraction patterns of specimens with different volume fraction of retained austenite (V_γ): (a) 14.8%, (b) 20.8%, (c) 41.0%.

3.6 Abrasion Wear Test

The surface roughness of test pieces are controlled less than $3\mu\text{m}$ using a grinding machine. The surface roughness is measured at three location using a roughness tester.

3.6.1 Suga wear test

A schematic drawing of an abrasion wear tester is illustrated in Fig.3-6. Under a load of 10 N (1kgf), the abrading wheel (44 mm in diameter and 12 mm in thickness) fixed by a 180 mesh SiC abrasive paper on the circumference is revolved intermittently, moving back and forth for 30 mm per one stroke on a same area of the test piece in dry condition. The revolving speed of the abrading wheel is 0.345 mm/s and the worn area is $360 (12 \times 30) \text{ mm}^2$. The abrading wheel rotates 0.9 degree by every one stroke. Therefore, it completely rotates one revolution or 360 degree after moving back and forth for 400 strokes. After testing, the specimen is cleaned with acetone in an ultrasonic cleaner and then dried. The weight loss of the test piece is measured using a high precision digital balance with 0.1 mg accuracy. The test is repeated up to eight times for one test piece.

3.6.2 Rubber wheel abrasion wear test

The schematic drawing of rubber wheel abrasion wear tester is shown in Fig.3-7. The silica sand of AFS 60 grade is used as the abrasives. The abrasives are fed into the contacting face between the rotating rubber wheel and a test piece. The test is conducted at a rotating speed of 120 rpm. The rate to feed the abrasives is approximate 250-300 g/ min. The load applied is 8.7 kgf. After the rubber wheel rotates for 1,000 revolutions, the specimen is taken out and cleaned with acetone in an ultrasonic cleaner

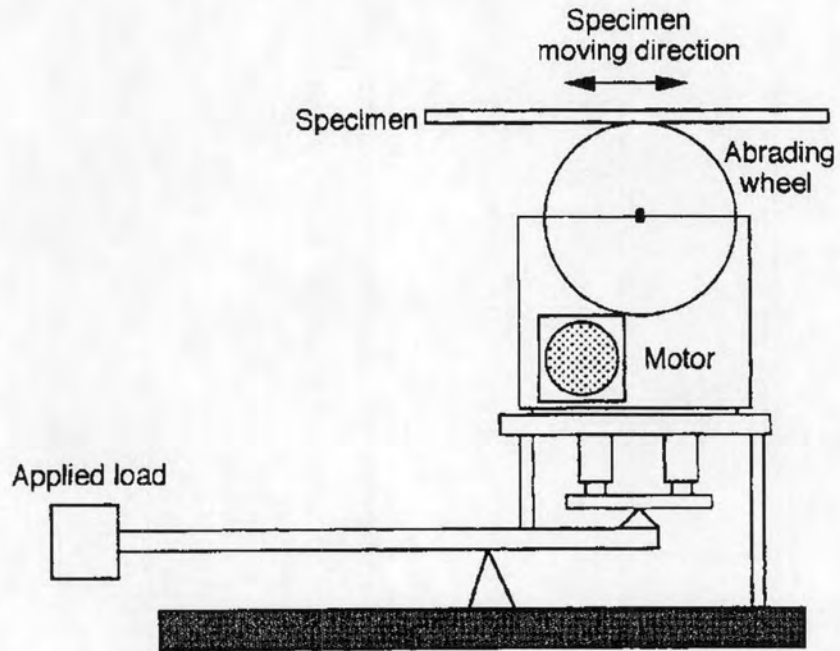


Fig.3-6 Schematic drawing of Suga abrasion wear tester.

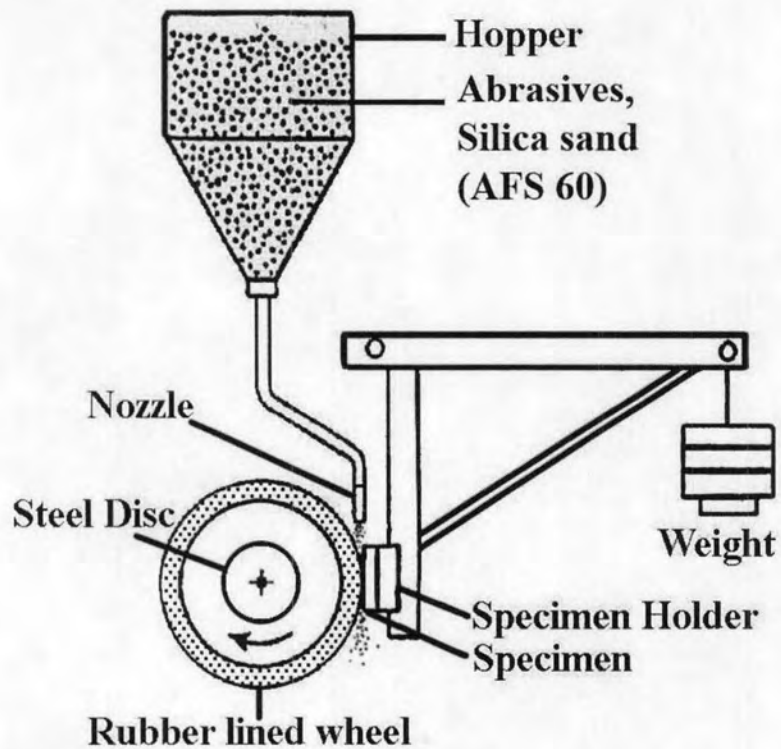


Fig.3-7 Schematic drawing of rubber wheel abrasion wear tester.

and then dried. The weight loss of the test piece is measured using a high precision digital balance with 0.1 mg accuracy. The test is repeated up to four times for one test piece.

Two abrasion wear tests are done and the average value of wear losses is adopted.

3.7 Abrasive

A particle or grit is usually used as an abrasive material because it can give a rapid or an efficient abrasion wear. Natural minerals have considerable hardness and abrasivity and then they are the main cause of abrasion wear problem in many parts and component in the industry. So, silicon carbide (SiC) with a hardness of 3000 VH (Vickers Hardness) or 30 GPa is availed as the abrasives in this study.

3.7.1 Abrasion paper for Suga abrasion wear test

The SEM microphotographs with different magnification of 180 mesh SiC abrasive paper used in Suga abrasion wear test are shown in Fig.3-8. The SiC abrasives, of which particle sizes are about 200 μm as shown in Fig.3-10, are fixed strongly to the paper by glue uniformly. Therefore, the abrasive particles cannot rotate during the test, and the tips of particles always scratch the surface of test piece

3.7.2 Silica sand for Rubber wheel abrasion wear test

SEM micro photographs with different magnification of silica sand of AFC 60 grade are shown in Fig.3-9. The size of silica sands are 500-700 μm , as shown in Fig.3-10.

Comparing with the SiC abrasives for Suga abrasion wear test, silica sand is much bigger, sharper and more angular. The abrasives of silica sand can move and roll freely on the surface of test piece.

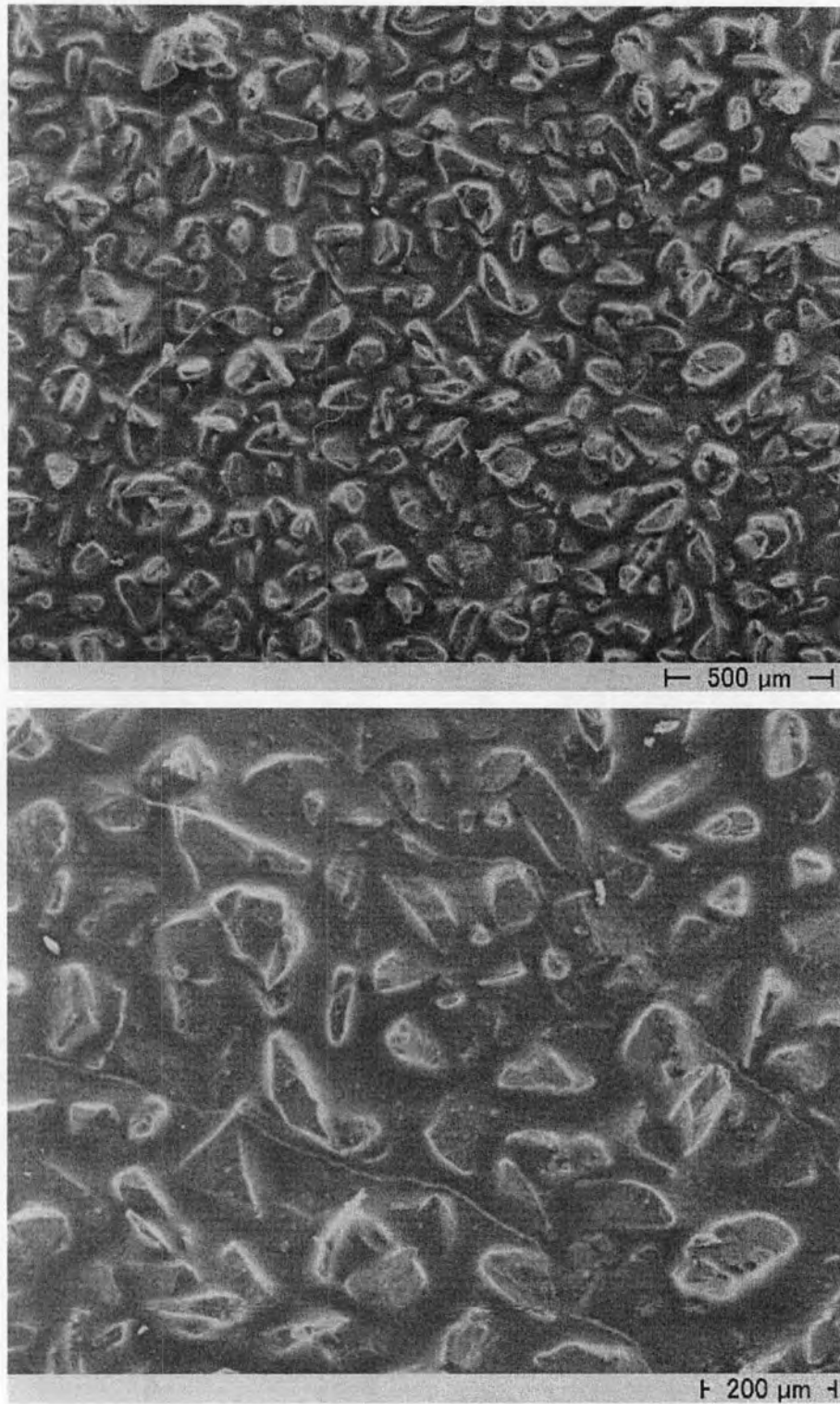


Fig.3-8 SEM microphotographs of abrasives for Suga abrasion wear test (180 mesh SiC abrasive paper).

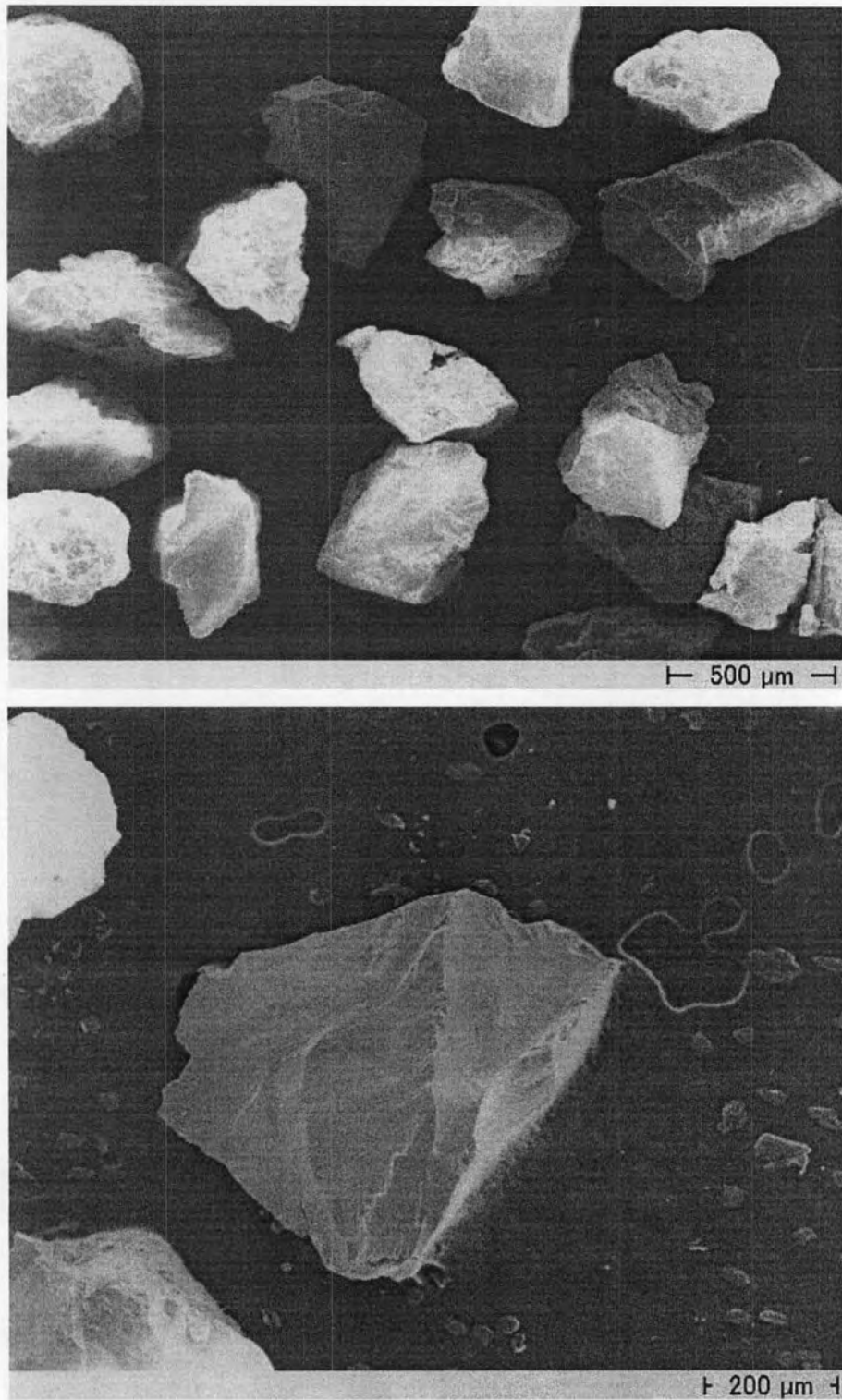
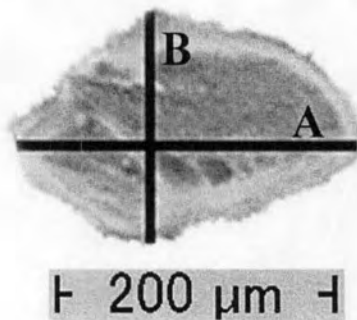


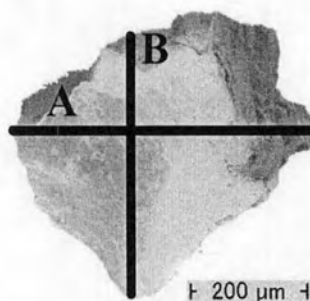
Fig.3-9 SEM microphotograph of silica sands of AFS 60 grade for Rubber wheel abrasion wear test.

3.7.3 Comparison of abrasive particles between 180 mesh SiC abrasive paper for Suga abrasion wear test and SiO₂ sand for Rubber wheel abrasion wear test

To express the criteria for comparing the size and shape of abrasive particles, a parameter of the aspect ratio is introduced for the shape or angularity and the schematic illustration of how to measure is shown in Fig.3-10 (a) for SiC and (b) for SiO₂ sand. The average values are obtained by measuring thirty abrasive particles and they are shown in table 3-6.



(a) SiC particle for Suga abrasion wear test



(b) SiO₂ sand for Rubber wheel abrasion wear test

Fig. 3-10 Schematic illustrations showing method to measure the aspect ratios of the abrasive particles of Suga and Rubber wheel wear tests.

Table 3-6 Comparison of size and angularity (aspect ratio) of the abrasive particles between 180 mesh SiC abrasive paper and SiO₂ sand with AFS 60 grade

Abrasives	Size (μm), [(A+B)/2]		Aspect ratio, [A/B]	
	Range	Average	Range	Average
SiC for Suga	62.50 – 155.00	91.83	1.00 – 8.33	2.35
SiO ₂ for Rubber wheel	258.17 – 513.07	363.83	1.01 – 3.89	1.44

From the results, the sizes of SiC particles are in range from 62.5 to 155.0 μm and the average is 91.8 μm . On the other hand, the size of SiO₂ sand range from 258.2 to 513.1 μm and the average is 363.8 μm . It is clear that the SiO₂ sand is around four times as big as the SiC particles. The shape or angularity of abrasive particles is expressed by the aspect ratio. The results show that the aspect ratio of SiC particles are in range from 1.00 to 8.33 and the average value is 2.35 μm , and those of SiO₂ sand range from 1.00 to 3.89 μm and the average size is 1.44 μm . The aspect ratio of SiC particle is 7 times as large as that of SiO₂ sand and this means that the SiC particles is longer and more angular than SiO₂ sand.